atmosphere

Article

Estimation of Forest Fire Emissions in Southwest China from 2013 to 2017

Wenjia Wang, Qixing Zhang *, Jie Luo, Ranran Zhao and Yongming Zhang *

State Key Laboratory of Fire Science, University of Science and Technology of China, Hefei 230026, China; wwjia@mail.ustc.edu.cn (W.W.); ajybfq@mail.ustc.edu.cn (J.L.); ranz2@mail.ustc.edu.cn (R.Z.)

* Correspondence: qixing@ustc.edu.cn (Q.Z.); zhangym@ustc.edu.cn (Y.Z.); Tel.: +86-551-6360-0770 (Q.Z.); +86-551-6360-6457 (Y.Z.)

Received: 21 November 2019; Accepted: 19 December 2019; Published: 22 December 2019

Abstract: Forest fire emissions have a great impact on local air quality and the global climate. However, the current and detailed regional forest fire emissions inventories remain poorly studied. Here we used Moderate Resolution Imaging Spectroradiometer (MODIS) data to estimate monthly emissions from forest fires at a spatial resolution of 500 m × 500 m in southwest China from 2013 to 2017. The spatial and seasonal variations of forest fire emissions were then analyzed at the provincial level. The results showed that the annual average emissions of CO_2, CO, CH_4, SO_2, NH_3, NO_X, PM, black carbon, organic carbon, and non-methane volatile organic compounds from forest fires were 1423.19×10^3, 91.66×10^3, 4517.08, 881.07, 1545.04, 1268.28, 9838.91, 685.55, 7949.48, and 12,724.04 Mg, respectively. The forest fire emissions characteristics were consistent with the characteristics of forest fires, which show great spatial and temporal diversity. Higher pollutant emissions were concentrated in Yunnan and Tibet, with peak emissions occurring in spring and winter. Our work provides a better understanding of the spatiotemporal representation of regional forest fire emissions and basic data for forest fire management departments and related research on pollution and emissions controls. This method will also provide guidance for other areas to develop high-resolution regional forest fire emissions inventories.

Keywords: forest fire emissions; MODIS; estimation; regional scale

1. Introduction

In terms of types of biomass burning, forest fires are the primary contributor to non-agricultural fire emissions in China [1,2]. Forest fires produce a large amount of trace gases and particulate matter worldwide, which worsen local and regional air quality and the global climate [3,4]. Future climate warming will increase the occurrence of forest fires, aggravating regional air quality and climate [5]. Therefore, forest fire emissions will account for a larger proportion of pollutant emissions.

Since the seminal work on biomass burning emissions [6,7], numerous research studies on the estimation of biomass emissions at different spatial and temporal resolutions have been carried out. Streets et al. [8] used a wide variety of sources to develop an inventory of biomass burning in Asia. In their estimations, activity data were obtained from official statistics. However, the national and provincial statistical data have inaccurate and unreliable for a variety of reasons [4,9] and provide less information on burned area. In recent years, with the wide application of satellite remote sensing technology, studies have developed an understanding of the spatial and temporal distributions of fire emissions using satellite data and Moderate Resolution Imaging Spectroradiometer (MODIS) products on emissions estimation. For example, the Global Fire Emission Database (GFED) [10,11] and the Fire INventory from NCAR(FINN) [12] showed that MODIS products exhibit an optimum performance in retrieving burned area, thus providing useful information.

Although they are an important type of biomass burning, forest fire emissions have been commonly analyzed only as a part of overall biomass burning emissions, and detailed analysis of the spatial and temporal changes of the forest fire emissions has been neglected [1,13–15]. Tian et al. [16,17] noted that forest fires are influenced by many factors and have more complex characteristics than other biomass types. Huang et al. [18] indicated that compared with forest fires, agricultural field burnings have small sizes and temporal impermanency. Few studies have aimed to differentiate the type of biomass burning and most typically focus on just emissions from forest fires. It is unreasonable to calculate forest fire emissions as a part of the total fire emissions because of their highly complex nature. For example, to simplify the calculations, a fixed biomass density or emission factor value has been applied for all forest types in many studies [13,19]. Above-ground biomass density values in different regions are quite different [2,20]. Therefore, it is necessary to use local biomass density to estimate regional forest fire emissions. Moreover, large uncertainties in the form of varied emission factor values can be found for different forest fuels in forest fire emissions estimation [20,21]. Therefore, the accurate estimation and detailed analysis of forest fire emissions still need to be improved.

Streets et al. [8] found that forest fire emissions were the primary source of biomass emissions in Asia, and that China had the highest biomass burning emissions in Asia. Some research has addressed forest fire emissions in China, but most of these studies have only estimated and analyzed the carbon emissions from forest fires [22,23]. Moreover, there is a lack of current and detailed regional forest fire emissions inventories. In China, forest fires mainly occur in the northeast and southwest regions [16]. To date, there have been few studies that could quantify detailed forest fire emissions inventories and provide analysis on spatio-temporal variation of pollutants emitted in southwest China. Wang et al. [24] estimated forest fire emissions in southwest China from 1959 to 1992 using statistical data. However, there are great interannual variations in forest fire emissions. Therefore, an inventory reflecting recent forest fire emissions is needed for regional forest fire management departments and research related to pollution and emission controls.

In this work, we used the MODIS data to develop updated emissions inventories for CO_2, CO, CH_4, SO_2, NH_3, NO_X, PM, black carbon (BC), organic carbon (OC), and non-methane volatile organic compounds (NMVOCs) from forest fires at a spatial resolution of 500 m × 500 m from 2013 to 2017 in southwest China. Based on this, we calculated cumulative emissions and annual emissions during the study period in this region. Circumstantial monthly emissions data and provincial annual emissions data for southwest China are listed in the Supplementary Material. We further examined the spatial and temporal variation of pollutant emissions from forest fires in different seasons and provinces based on the emission inventories. The distribution of forest fire emissions in southwest China was explored in more detail by combining the characteristics of forest fires. The results of this study are compared to previous reports, and the uncertainties are discussed.

2. Methods

2.1. Emission Calculation

Southwest China refers specifically to Yunnan province, Guizhou province, Tibet (Xizang province), Sichuan province, and Chongqing province in this work, which includes one of the three largest forest areas in China. Forest fire emissions from each province in southwest China were estimated using the bottom-up method developed by Seiler and Crutzen et al. [7]:

$$E_{m,i} = \sum_{j} BA_{m,j} \times BD_{m,j} \times BE_j \times EF_{i,j} \quad (1)$$

where $E_{m,i}$ denotes the emissions of species i in m province, $BA_{m,j}$ is the burned area (ha) in m province for the j forest cover type, $BD_{m,j}$ is the aboveground biomass density (Mg/ha) in m province for the j forest cover type, BE_j is the burning efficiency for the j forest cover type, $EF_{i,j}$ is the emission factor of species i for the j forest cover type (g kg^{-1}).

2.2. Forest Cover

Vegetation classification is one of the most important sources of information for forest fire emissions calculation, as different forest types have different values of biomass density and emission factors [11,15]. In this study, a forest cover map was obtained from the Collection 6 MODIS land cover product (MCD12Q1 v006), which had a 500 m × 500 m spatial resolution and yearly temporal resolution. The data were obtained from the NASA Land Process Distributed Active Archive Center, USA (https://lpdaac.usgs.gov). The 14-class University of Maryland classification (UMD) was used for the forest cover classification legends. Qiu et al. [13] used the vegetation map of the People's Republic of China that was published in 2007 to estimate the open biomass burning emissions in China, although it ignores interannual dynamics in land cover properties. We obtained the forest cover type maps from MCD12Q1 for each year from 2013 to 2017 for emission estimation. Figure 1 shows the forest cover maps for southwest China in 2013.

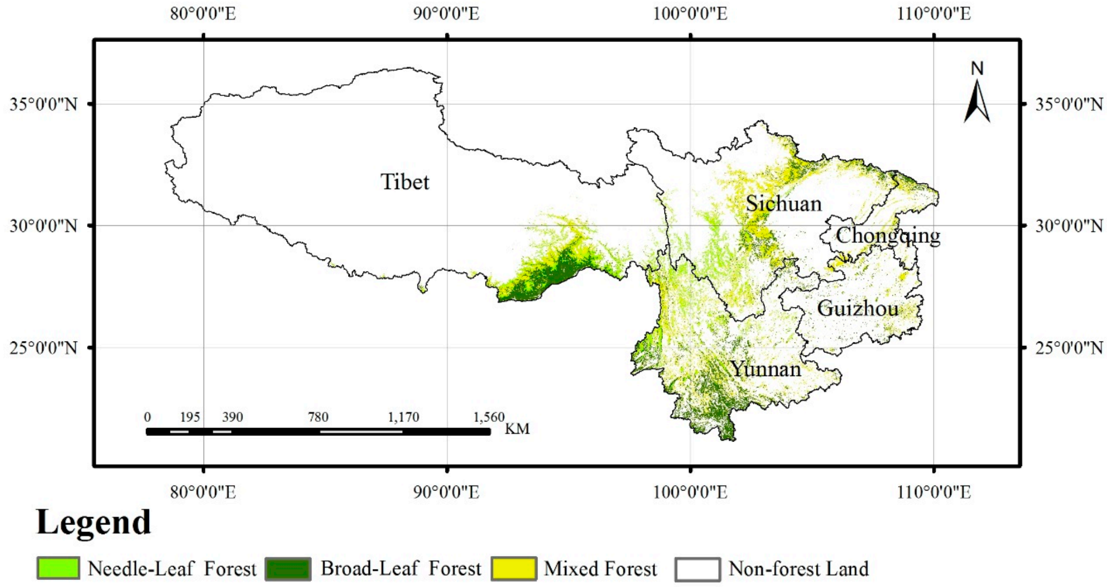

Figure 1. Distribution of forest types in southwest China in 2013.

2.3. Burned Area

To establish the emission inventories with a high resolution, we derived burned area maps using the Collection 6 MODIS Burned Area product data (MCD64A1 v006). MCD64A1 uses surface reflectance, daily active fire, and land cover products to map the burned areas at a 500 m × 500 m spatial resolution and monthly temporal resolution [25,26]. We extracted the overlapping grids from burned area maps and forest cover maps to create monthly forest burned area maps. From these, we obtained the monthly burned area maps of different forest types. We added up the burned area grids of the same forest types and calculated the value of the burned area in the same forest types based on the number of grids. Figure 2 shows the whole year of forest fire burned area grids in southwest China in 2013.

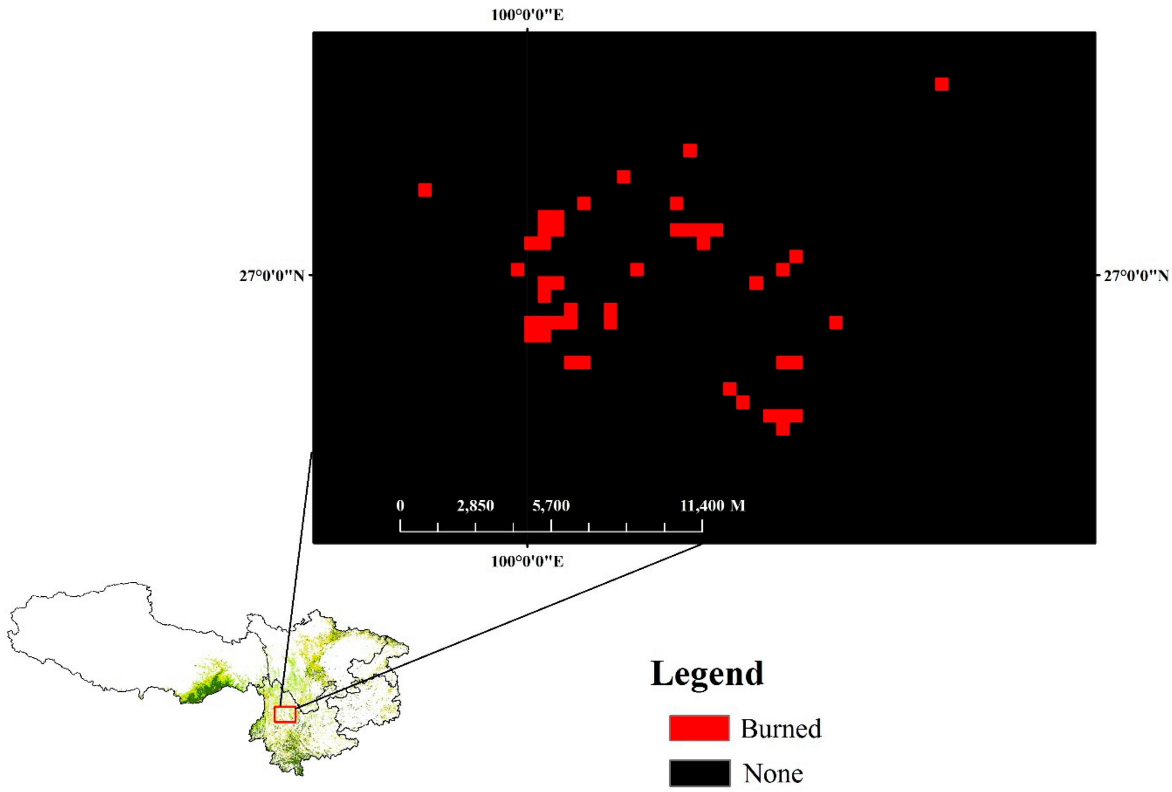

Figure 2. The forest burned area grids in southwest China in 2013.

2.4. Biomass Density and Burning Efficiency

The values of aboveground biomass density were based on research on province-specific aboveground biomass density in China for various forest types [20,21], as shown in Table 1, which came from direct field measurements and reflected spatial variations in forest type.

Table 1. Aboveground biomass density assigned at the provincial level in China.

Description	Yunnan	Guizhou	Tibet	Sichuan	Chongqing
	Unit: Mg/ha				
Needle-leaved forest	57.6	22.1	139.9	80.9	80.9
Broad-leaved forest	145.1	114.1	64.9	99	99
Mixed forest	101.35	68.1	102.4	89.95	89.95

Burning efficiency is an uncertain parameter in fire emissions estimation due to the high-spatial variability of both the burning process and fuel availability, and it has usually been set as a constant in previous works [9,12,27]. In this paper, specific forest types were derived from MCD12Q1 data, and the burning efficiency of all forest types was defined as a constant value of 0.25 according to the report of Michel et al. [28]. The value was based on a review that summarized several studies of the UMD vegetation classes.

2.5. Emission Factors

Emission factors vary greatly at different stages of combustion, and the impact of different biomasses on emission factors is complex [2]. Limited information is available on the emission factors for forest fires in southwest China. The latest emission factors data were collected experimentally in China, which was the preferred method in other relevant research. In this study, the same emission factor values were applied to the same forest type according to the extensive literature reviews by

Song et al. [2] and Wu et al. [1]. The emission factors of forest fires for each pollutant are summarized in Table 2.

Table 2. Emission factors assigned to forest fires in each of the forest types from the MCD12Q1 data (unit: g kg^{-1}). BC: black carbon; OC: organic carbon; NMVOCs: non-methane volatile organic compounds.

Description	CO_2	CO	CH_4	SO_2	NH_3	NO_X	PM	BC	OC	$NMVOC_S$
Needle-leaved forest	1514	118	6	1	3.5	2.4	9.7	0.80	7.8	28
Broad-leaved forest	1630	102	5	1	1.5	1.3	13	0.77	9.2	11
Mixed forest	1630	102	5	1	1.5	1.3	9.7	0.78	9.2	14

3. Results and Discussion

3.1. Emission Inventory of Forest Fires in 2017

The annual emissions of CO_2, CO, CH_4, SO_2, NH_3, NO_X, PM2.5, BC, OC, and NMVOCs were 767,610, 50,390, 2491.88, 478.13, 919.66, 732.92, 5358.52, 372.78, 4257.07, and 7455.90 Mg, respectively, in 2017. We established emissions inventories of forest fires in southwest China in 2017 (Table 3). Southwest China has a subtropical monsoon climate with high temperatures and rainy summers, which may lead to some months typically having no forest fires [29]. The burnt area of forest obtained from MCD64A1 had a zero range from June to October in 2017, therefore, emissions for the corresponding months were zero. Having a burnt forest area of zero means that there were no forest fires or that there were just a very few small fires that can be ignored and were missing in the data for MCD64A1. Table 3 also shows that forest fire emissions mainly occurred in spring and winter in southwest China in 2017, and almost 88% of emissions were observed in February and March. In addition, the forest area sizes of each province in southwest China in 2017 are shown in Table 4, which were obtained from MCD12Q1.

Table 3. Monthly forest fire emissions for each pollutant in 2017 (units: Mg).

	CO_2	CO	CH_4	SO_2	NH_3	NO_X	PM2.5	BC	OC	$NMVOC_S$
January	64.78×10^3	4.68×10^3	235.44	41.67	116.69	83.97	424.36	32.98	345.44	944.31
February	496.74×10^3	32.06×10^3	1580.57	307.73	545.44	446.16	3470.08	239.40	2772.43	4454.10
March	176.60×10^3	11.75×10^3	582.65	110.49	226.14	176.86	1269.17	86.19	974.23	1790.23
April	18.44×10^3	1.15×10^3	56.55	11.31	16.97	14.70	115.68	8.80	104.05	152.91
May	7.04×10^3	0.49×10^3	24.32	4.46	10.73	8.02	49.24	3.50	38.20	85.29
June	0	0	0	0	0	0	0	0	0	0
July	0	0	0	0	0	0	0	0	0	0
August	0	0	0	0	0	0	0	0	0	0
September	0	0	0	0	0	0	0	0	0	0
October	0	0	0	0	0	0	0	0	0	0
November	0.67×10^3	0.04×10^3	2.05	0.41	0.62	0.53	5.33	0.32	3.77	4.51
December	3.36×10^3	0.21×10^3	10.30	2.06	3.09	2.68	24.70	1.59	18.95	24.55
Total	767.61×10^3	50.39×10^3	2491.88	478.13	919.66	732.92	5358.52	372.78	4257.07	7455.90

Table 4. Forest area size of each province in Southwest China in 2017 (unit: ha).

Tibet	Yunnan	Guizhou	Sichuan	Chongqing
8.3×10^6	14.0×10^6	2.4×10^6	11.2×10^6	1.6×10^6

The proportions of each of the pollutants in the forest fire emissions of different provinces are shown in Figure 3. We merged Chongqing and Sichuan province for calculation and analysis, because they have same value of aboveground biomass density. Additionally, Chongqing had very little burnt forest area during the study period. Tibet had the highest emissions, which accounted for the maximum ratio of emissions for all pollutants, 54.79%–62.95%. The smallest forest fire emissions were observed in Guizhou province, which contributed only 0.74%–1.08% of the total forest fire pollutant emissions. The other provinces of Yunnan and Sichuan and Chongqing accounted from 25.99%–28.43% and 9.61%–16.96% of the total, respectively.

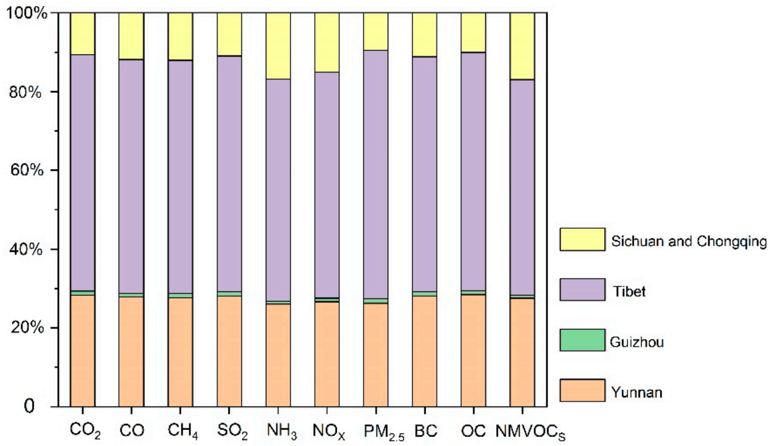

Figure 3. The pollutant emissions contribution of different provinces in southwest China in 2017.

Here, CO was used as an example to analyze the seasonal variations of emissions in 2017, because CO was widely studied in open fire emission modeling [8,30]. From Figure 4, it can be noted that CO emissions from forest fires were mainly observed between December and May in Yunnan, while the CO emissions only appeared in December and February in Guizhou. For Tibet and Sichuan and Chongqing, the monthly distributions of CO emissions were also different. The largest emissions of CO in Yunnan, Tibet, and Guizhou occurred in February and accounted for 72% of annual emissions. However, in Sichuan and Chongqing, the largest emissions occurred in March, while the emissions in February only accounted for less than 2% of the year. It can be concluded that monthly variations of CO emissions for the provinces were very significant in 2017. Therefore, in terms of forest fire emissions controlling, each province should take corresponding measures based on its own historical data and situation.

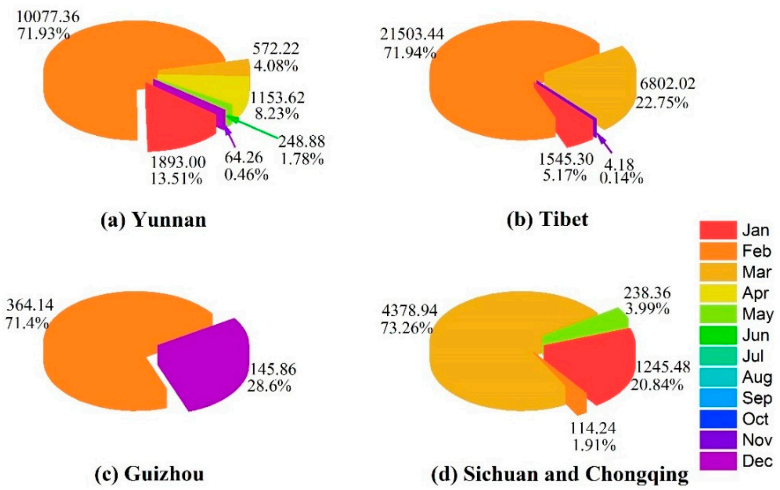

Figure 4. The monthly CO emissions of the provinces in southwest China in 2017 (units: Mg). (**a**) CO emissions in Yunnan, (**b**) CO emissions in Tibet, (**c**) CO emissions in Guizhou, (**d**) CO emissions in Sichuan and Chongqing.

3.2. Historical Emission Inventories of Forest Burning

The cumulative emissions of CO_2, CO, CH_4, SO_2, NH_3, NO_X, PM2.5, BC, OC, and $NMVOC_S$ were 7115.95×10^3, 458.29×10^3, 22,585.42, 4405.37, 7725.22, 6341.41, 49,194.55, 3427.77, 39,747.4, and 63,620.2 Mg, respectively, from 2013 to 2017. Complete annual forest fire emission inventories in southwest China and the annual forest fire emissions of each province are shown in the Supplementary Material. The annual emissions from forest fires varied greatly in southwest China, as shown in Figure 5. Emissions exhibited interannual oscillation from 2013 to 2017, with the highest emissions in 2014 and lower emissions in 2015 and 2017. An irregular increase or decrease over the years can be observed, which can be explained by the random yearly variation of emissions in each province. Forest fires were influenced by many factors and each province has different dominant factors and variables, which largely account for the random yearly variation of emissions of different provinces. Therefore, the variations of emissions from 2013 to 2017, rather than the overall trend for the whole period, are discussed in this work. In addition, the forest fire emissions in southwest China showed strong spatial differences. The different provinces show significant differences in annual emissions variations in Figure 5, which also illustrates the great spatial diversity of forest fire emissions in southwest China.

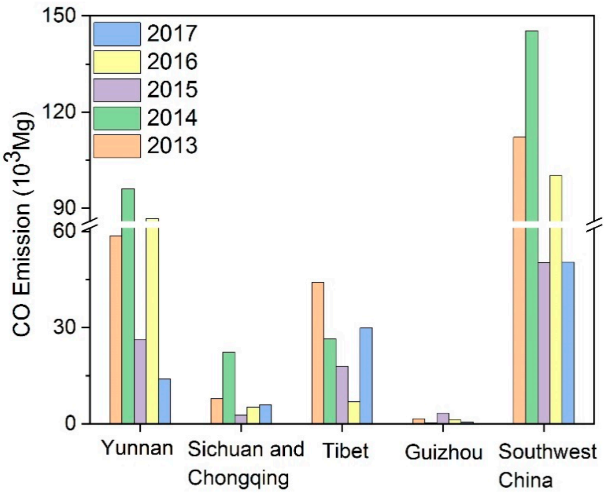

Figure 5. CO emissions of forest fires from 2013 to 2017 in southwest China.

The proportion of annual average forest fire emissions from different provinces are presented in Figure 6, which shows that Yunnan and Tibet had the most forest fire emissions in southwest China in the past five years. The emission contribution of Guizhou province was relatively small. Over half of the annual average total emissions came from Yunnan from 2013 to 2017. This may not only be due to the greater forest cover in Yunnan province. Although the forest coverage of Sichuan and Chongqing is second only to that of Yunnan, their forest fire emissions were lower than that of Tibet. Therefore, more factors affecting forest fire emissions need to be further studied.

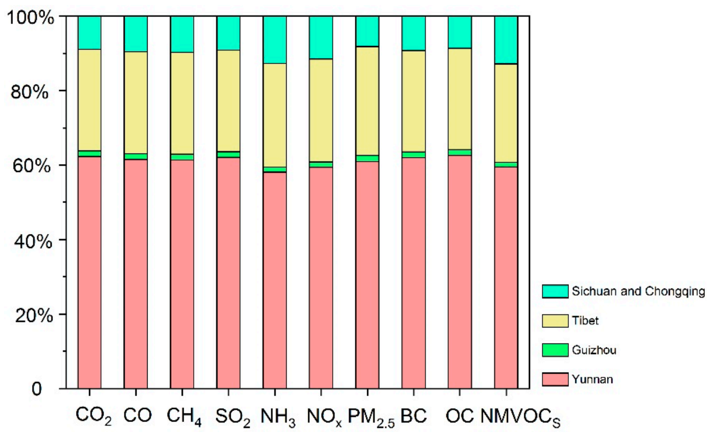

Figure 6. The annual average contributions of forest fire emissions in each province from 2013 to 2017.

It also should be noted that the official data from the China Forestry Yearbooks and China Forestry Statistical Yearbooks showed that the average annual proportion of forest burned area in Tibet was less than 1% of that in southwest China. However, the results from this work are consistent with the work of Yin et al. [31], which notably showed that the annual average forest fire emissions in Tibet are second only to those in Yunnan. The great uncertainties of the official statistics should not be overlooked and Tibet, in particular, contains many remote and sparsely populated areas [4]. Therefore, more attention should be paid to the monitoring and management of forest fire emissions in Tibet.

All the pollutants had similar temporal and spatial variations in their emission trends. CO was chosen as a representative pollutant to demonstrate the seasonal emission variations over the past five years. Figure 7 presents the cumulative CO emissions of each season from 2013 to 2017. High CO emissions were observed in spring and winter, while only a small amount of emissions occurred in summer and autumn. The temporal characteristics of forest fire emissions are consistent with the temporal characteristics of forest fires. For Yunnan province, which is the largest contributor to forest fire emissions in southwest China, the monthly CO emissions from forest fires from 2013 to 2017 are shown in Figure 8. According to previous studies, the forest fires in Yunnan province are distributed from November to June of the following year, concentrated in January to May, with peaks around March. The peak in the number of forest fires around March each year is also related to the existence of traditional festivals, such as Qingming, at this time. This is consistent with the temporal characteristics of forest fire emissions in Yunnan. Figure 9 illustrates the monthly trend of CO emissions from 2013 to 2017. It shows that the highest emissions occurrences were predominantly in different months in different years, but that peaks may occur from January to April. In contrast, the amount of emissions from June to November was always very small. Therefore, the enforcement and effective control of forest fires in southwest China during January to April is important for improving regional air quality.

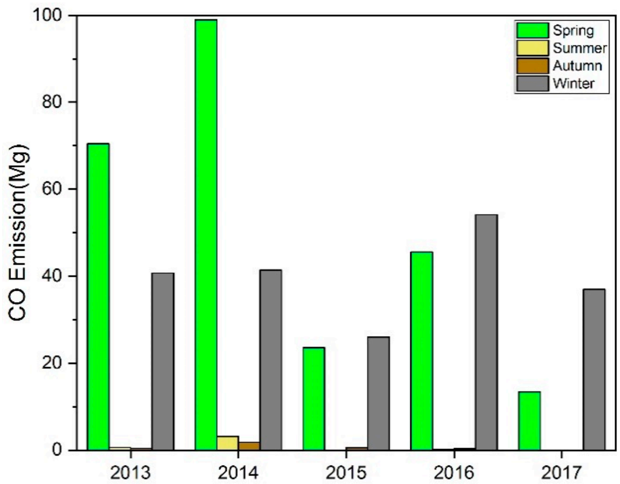

Figure 7. Seasonal distribution of CO emissions from forest fires in southwest China from 2013 to 2017. Spring: March–May; summer: June–August; autumn: September–November; winter: December–February.

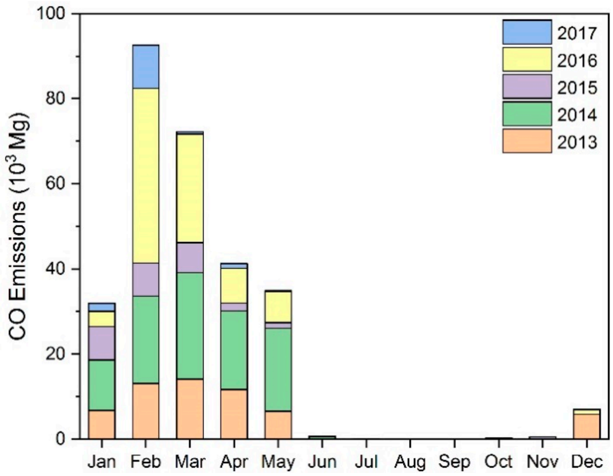

Figure 8. Monthly CO emissions of forest fires from 2013 to 2017 in Yunnan.

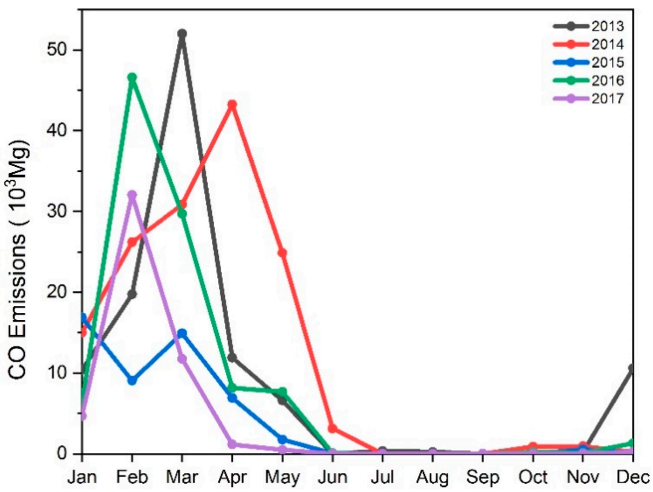

Figure 9. Monthly CO emissions of forest fires from 2013 to 2017 in southwest China.

3.3. Comparison with Other Emission Inventories

Emissions from forest fires in southwest China have been estimated in several publications. A comparison of the calculated emissions in our study with previous estimations is shown in Table 5. We proposed that the forest fires referred to fires with large burned areas, thus small fires were not considered. In this study, if a fire event detected by MODIS sensor was located in one 500 m × 500 m forest pixel in the forest cover map, it could be recognized as a forest fire.

Table 5. Comparison of the emissions with previous estimates at different temporal scales (unit: Mg).

Literature Cited	Period	CO_2	CO	CH_4
Wang et al. (2001) [24]	1959–1992	2053.62×10^3	259.39×10^3	25,399
This study	2013–2017	1423.19×10^3	91.66×10^3	4517.08
Qiu et al. (2016) [13]	2013	3831×10^3	299×10^3	15,200
This study	2013	1729×10^3	112×10^3	5537

The forest fire emissions for each pollutant estimated in this study were lower than previous works (Table 4). One of the important factors influencing the result was the forest cover map. Magdon et al. [32] proposed that as forests are highly diverse and complex, it is hard to give a quantitative and comprehensive definition of a forest. At the national level, different variations of forest definitions are in use [32,33]. Forest definitions delineate forest land and non-forest land. This study derived the forest cover map from MCD12Q1, and the UMD legend and class definitions were used, which described a forest as an area with tree cover over 0.6. However, the China Statistical Yearbook on Environment (2018) defined a forest as an area with a canopy density greater than 0.2. Using the UMD classification method and Chinese forest classification method, the forest area in southwest China in 2013 was 34.348 million ha and 57.8274 million ha, respectively. Differences with the previous studies mainly come from two aspects: (1) interannual forest cover maps were used for calculation, which reduced errors from interannual changes in forest vegetation cover; and (2) more precise parameters were used to calculate the forest fire emissions in our work. For example, we used province-specific aboveground biomass densities for various forest types and preferred to use the latest emission factors data that were collected experimentally in China.

3.4. Limitations and Uncertainties

The uncertainties of the estimated forest fire emissions arise from the forest burned area, biomass density, burning efficiency, and emission factors. Forest burned area was derived from MCD64A1 and MCD12Q1. The algorithm of MCD64A1 is more tolerant of cloud and aerosol contamination, but information regarding burn data is still lacking for some areas due to insufficient data [25]. Lack of an experimental methodology and field data for different forest components in various ecosystems made it difficult to obtain an accurate aboveground biomass density value. In addition, the required use of generalized burning efficiencies and approximate experimental measurements of emission factors also contribute to the existence of estimation uncertainties [34].

Despite these uncertainties, this study combined the MODIS burned area product and land cover product to obtain an accurate map of the burned area of different forest types. Moreover, the province-specific aboveground biomass density and forest type-specific emission factor values also helped us to improve the accuracy of the emission inventories.

4. Conclusions

In summary, we estimated monthly emissions from forest fires in southwest China at a 500 m × 500 m resolution from 2013 to 2017 based on MODIS data. The results suggested that annual average CO_2, CO, CH_4, SO_2, NH_3, NO_X, PM2.5, BC, OC, and $NMVOC_S$ emissions from forest fire were 1423.19×10^3, 91.66×10^3, 4517.08, 881.07, 1545.04, 1268.28, 9838.91, 685.55, 7949.48, and 12,724.04 Mg, respectively. The forest fire emissions in southwest China showed great spatial diversity, because forest fires are influenced by many factors and each province had different dominant factors and variables. Yunnan was the largest contributor to forest fire emissions in southwest China. Importantly, the results demonstrated that the annual average forest fire emissions in Tibet were second only to those in Yunnan. The temporal characteristics of forest fire emissions were consistent with the temporal characteristics of forest fires. Forest fire emissions were highly concentrated in spring and winter in southwest China. Additionally, the monthly variation of emissions for different years varied, and the emissions peaks of different years ranged from January to April. In contrast, there were few emissions from June to November. Therefore, the enforced and effective control of forest fires in southwest China during January to April is important for improving regional air quality.

The estimation of multi-year regional forest fire emissions by MODIS data in this study provides objective and credible evidence for understanding the spatiotemporal representation of forest fire emissions in southwest China. The high-spatial-resolution emission inventories at a monthly scale also provide useful basic data for regional forest fire management departments and research related to pollution and emission controls.

Supplementary Materials: The following are available online at http://www.mdpi.com/2073-4433/11/1/15/s1: Forest fire emission inventories of southwest China from 2013 to 2017 (Tables S1–S5); Provincial forest fire emission inventories of southwest China from 2013 to 2017 (Tables S6–S10).

Author Contributions: W.W. and Q.Z. designed the study. W.W., Q.Z., J.L., and R.Z. performed the data analysis and discussed the results. Q.Z. and Y.Z. supervised the project. W.W. prepared the manuscript with contributions from all co-authors. All authors have read and agreed to the published version of the manuscript.

Funding: This research was funded by the National Key Research and Development Plan grant number 2016YFC0800100, the National Natural Science Foundation of China grant number 41675024, and Fundamental Research Funds for the Central Universities grant number WK2320000040.

Conflicts of Interest: The authors declare no conflict of interest.

References

1. Wu, J.; Kong, S.; Wu, F.; Cheng, Y.; Zheng, S.; Yan, Q.; Zheng, H.; Yang, G.; Zheng, M.; Liu, D.; et al. Estimating the open biomass burning emissions in central and eastern China from 2003 to 2015 based on satellite observation. *Atmos. Chem. Phys.* **2018**, *18*, 11623–11646. [CrossRef]
2. Song, Y.; Liu, B.; Miao, W.; Chang, D.; Zhang, Y. Spatiotemporal variation in nonagricultural open fire emissions in China from 2000 to 2007. *Glob. Biogeochem. Cycles* **2009**, 23. [CrossRef]
3. Andreae, M.O. Biomass burnin—Its history, use, and distribution and its impact onenvironmental quality and global climate. In *Global Biomass Burning—Atmospheric, Climatic, and Biospheric Implications*; MIT Press: Cambridge, UK, 1991; pp. 3–21.
4. Li, J.; Song, Y.; Huang, X.; Li, M. Comparison of forest burned areas in mainland China derived from MCD45A1 and data recorded in yearbooks from 2001 to 2011. *Int. J. Wildland Fire* **2015**, *24*, 103–113. [CrossRef]
5. Lazaridis, M.; Latos, M.; Aleksandropoulou, V.; Hov, Ø.; Papayannis, A.; Tørseth, K. Contribution of forest fire emissions to atmospheric pollution in Greece. *Air Qual. Atmos. Health* **2008**, *1*, 143–158. [CrossRef]
6. Crutzen, P.J.; Heidt, L.E.; Krasnec, J.P.; Pollock, W.H.; Seiler, W. Biomass burning as a source of atmospheric gases CO, H_2, N_2O, NO, CH_3Cl and COS. *Nature* **1979**, *282*, 253–256. [CrossRef]
7. Seiler, W.; Crutzen, P.J. Estimates of Gross and Net Fluxes of Carbon between the Biosphere and the Atmosphere from Biomass Burning. *Clim. Chang.* **1980**, *2*, 207–247. [CrossRef]
8. Streets, D.G.; Yarber, K.F.; Woo, J.H.; Carmichael, G.R. Biomass burning in Asia: Annual and seasonal estimates and atmospheric emissions. *Glob. Biogeochem. Cycles* **2003**, 17. [CrossRef]
9. Yan, X.; Ohara, T.; Akimoto, H. Bottom-up estimate of biomass burning in mainland China. *Atmos. Environ.* **2006**, *40*, 5262–5273. [CrossRef]
10. Randerson, J.T.; Chen, Y.; van der Werf, G.R.; Rogers, B.M.; Morton, D.C. Global burned area and biomass burning emissions from small fires. *J. Geophys. Res. Biogeosci.* **2012**, 117. [CrossRef]
11. Giglio, L.; Randerson, J.T.; van der Werf, G.R. Analysis of daily, monthly, and annual burned area using the fourth-generation global fire emissions database (GFED4). *J. Geophys. Res. Biogeosci.* **2013**, *118*, 317–328. [CrossRef]
12. Wiedinmyer, C.; Akagi, S.K.; Yokelson, R.J.; Emmons, L.K.; Al-Saadi, J.A.; Orlando, J.J.; Soja, A.J. The Fire INventory from NCAR (FINN): A high resolution global model to estimate the emissions from open burning. *Geosci. Model Dev.* **2011**, *4*, 625–641. [CrossRef]
13. Qiu, X.; Duan, L.; Chai, F.; Wang, S.; Yu, Q.; Wang, S. Deriving High-Resolution Emission Inventory of Open Biomass Burning in China based on Satellite Observations. *Environ. Sci. Technol.* **2016**, *50*, 11779–11786. [CrossRef] [PubMed]
14. van der Werf, G.R.; Randerson, J.T.; Giglio, L.; van Leeuwen, T.T.; Chen, Y.; Rogers, B.M.; Mu, M.; van Marle, M.J.E.; Morton, D.C.; Collatz, G.J.; et al. Global fire emissions estimates during 1997–2016. *Earth Syst. Sci. Data* **2017**, *9*, 697–720. [CrossRef]
15. Zhou, Y.; Xing, X.; Lang, J.; Chen, D.; Cheng, S.; Wei, L.; Wei, X.; Liu, C. A comprehensive biomass burning emission inventory with high spatial and temporal resolution in China. *Atmos. Chem. Phys.* **2017**, *17*, 2839–2864. [CrossRef]
16. Tian, X.; Zhao, F.; Shu, L.; Wang, M. Distribution characteristics and the influence factors of forest fires in China. *For. Ecol. Manag.* **2013**, *310*, 460–467. [CrossRef]
17. Ying, L.X.; Han, J.; Du, Y.S.; Shen, Z.H. Forest fire characteristics in China: Spatial patterns and determinants with thresholds. *For. Ecol. Manag.* **2018**, *424*, 345–354. [CrossRef]

18. Huang, X.; Li, M.; Li, J.; Song, Y. A high-resolution emission inventory of crop burning in fields in China based on MODIS Thermal Anomalies/Fire products. *Atmos. Environ.* **2012**, *50*, 9–15. [CrossRef]
19. Qin, Y.; Xie, S.D. Historical estimation of carbonaceous aerosol emissions from biomass open burning in China for the period 1990–2005. *Environ. Pollut.* **2011**, *159*, 3316–3323. [CrossRef]
20. Fang, J.-Y.; Wang, G.G.; Liu, G.-H.; Xu, S.-L. Forest Biomass of China: An Estimate Based on the Biomass-Volume Relationship. *Ecol. Appl.* **1998**, *8*, 1084–1091. [CrossRef]
21. Fang, J.Y.; Liu, G.H.; Xu, S.L. Biomass and net production of forest vegetation in China. *Acta Ecol. Sin.* **1996**, *16*, 497–508.
22. Lü, A.; Tian, H.; Liu, M.; Liu, J.; Melillo, J.M. Spatial and temporal patterns of carbon emissions from forest fires in China from 1950 to 2000. *J. Geophys. Res.* **2006**, 111. [CrossRef]
23. Zhang, Y.; Qin, D.; Yuan, W.; Jia, B. Historical trends of forest fires and carbon emissions in China from 1988 to 2012. *J. Geophys. Res. Biogeosci.* **2016**, *121*, 2506–2517. [CrossRef]
24. Wang, X.; Feng, Z.; Zhuang, Y. CO_2, CO and CH_4 emissions from forest fires in China. *Sci. Silvae Sin.* **2001**, *37*, 90–95. (In Chinese)
25. Giglio, L.; Loboda, T.; Roy, D.P.; Quayle, B.; Justice, C.O. An active-fire based burned area mapping algorithm for the MODIS sensor. *Remote Sens. Environ.* **2009**, *113*, 408–420. [CrossRef]
26. Shi, Y.; Matsunaga, T.; Yamaguchi, Y. High-Resolution Mapping of Biomass Burning Emissions in Three Tropical Regions. *Environ. Sci. Technol.* **2015**, *49*, 10806–10814. [CrossRef]
27. Yi, K.; Bao, Y. Estimates of Wildfire Emissions in Boreal Forests of China. *Forests* **2016**, *7*, 158. [CrossRef]
28. Michel, C.; Liousse, C.; Gregoire, J.M.; Tansey, K.; Carmichael, G.R.; Woo, J.H. Biomass burning emission inventory from burnt area data given by the SPOT-VEGETATION system in the frame of TRACE-P and ACE-Asia campaigns. *J. Geophys. Res. Atmos.* **2005**, 110. [CrossRef]
29. Lu, A.F. Study on the relationship among forest fire, temperature and precipitation and its spatial-temporal variability in China. *Agric. Sci. Technol. Hunan* **2011**, *12*, 1396–1400.
30. Li, J.; Li, Y.; Bo, Y.; Xie, S. High-resolution historical emission inventories of crop residue burning in fields in China for the period 1990–2013. *Atmos. Environ.* **2016**, *138*, 152–161. [CrossRef]
31. Yin, L.; Du, P.; Zhang, M.; Liu, M.; Xu, T.; Song, Y. Estimation of emissions from biomass burning in China (2003–2017) based on MODIS fire radiative energy data. *Biogeosciences* **2019**, *16*, 1629–1640. [CrossRef]
32. Magdon, P.; Fischer, C.; Fuchs, H.; Kleinn, C. Translating criteria of international forest definitions into remote sensing image analysis. *Remote Sens. Environ.* **2014**, *149*, 252–262. [CrossRef]
33. Tomppo, E.; Gschwantner, T.; Lawrence, M.; McRoberts, R.E.; Gabler, K.; Schadauer, K.; Vidal, C.; Lanz, A.; Ståhl, G.; Cienciala, E. *National Forest Inventories*; Pathways for Common Reporting; European Science Foundation: Strasbourg, France, 2010; pp. 541–553.
34. Hao, W.M.; Petkov, A.; Nordgren, B.L.; Corley, R.E.; Silverstein, R.P.; Urbanski, S.P.; Evangeliou, N.; Balkanski, Y.; Kinder, B.L. Daily black carbon emissions from fires in northern Eurasia for 2002–2015. *Geosci. Model Dev.* **2016**, *9*, 4461–4474. [CrossRef]